



Hepatocyte-specific damage in acute toxicity of sodium ferrous citrate: Presentation of a human autopsy case and experimental results in mice

Yuji Nishikawa^{a,*}, Yasuhiro Matsuo^a, Ryosuke Watanabe^a, Mitsuyuki Miyazato^a, Mikiko Matsuo^a, Yasuharu Nagahama^a, Hiroki Tanaka^a, Takako Ooshio^b, Masanori Goto^a, Yoko Okada^a, Satoshi Fujita^c

^a Division of Tumor Pathology, Department of Pathology, Asahikawa Medical University, Asahikawa, Hokkaido 078-8510, Japan

^b Division of Biomedical Oncology, Institute for Genetic Medicine, Hokkaido University, Sapporo, Hokkaido 060-0815, Japan

^c Department of Emergency Medicine, Nayoro City General Hospital, Nayoro, Hokkaido 096-8511, Japan

ARTICLE INFO

Handling Editor: Dr. L.H. Lash

Keywords:

Iron poisoning
Oxidative stress
Cell death
Hepatocytes
Bile ducts

ABSTRACT

Acute iron overload is known to exert deleterious effects in the liver, but detailed pathology has yet to be documented. Here, we report pathological findings in an autopsy case of acute iron toxicity and validation of the findings in mouse experiments. In a 39-year-old woman who intentionally ingested a large amount of sodium ferrous citrate (equivalent to 7.5 g of iron), severe disturbance of consciousness and fulminant hepatic failure rapidly developed. Liver failure was refractory to treatment and the patient died on Day 13. Autopsy revealed almost complete loss of hepatocytes, while bile ducts were spared. To examine the detailed pathologic processes induced by excessive iron, mice were orally administered equivalent doses of ferrous citrate. Plasma aminotransferase levels markedly increased after 6 h, which was preceded by increased plasma iron levels. Hepatocytes were selectively damaged, with more prominent damage in the periportal area. Phosphorylated c-Jun was detected in hepatocyte nuclei after 3 h, which was followed by the appearance of γ -H2AX expression. Hepatocyte injury in mice was associated with the expression of Myc and p53 after 12 and 24 h, respectively. Even at lethal doses, the bile ducts were morphologically intact and fully viable. Our findings indicate that acute iron overload induces hepatocyte-specific liver injury, most likely through hydroxyl radical-mediated DNA damage and subsequent stress responses.

1. Introduction

Acute iron poisoning has been demonstrated to induce liver injury as a dose-related phenomenon [1]. The majority of human cases, sometimes lethal, have been encountered as accidental overdoses of ferrous sulfate in children [2–6], as ferrous sulfate is the most commonly used iron supplement available over the counter. However, it is important to note that intentional overdose of ferrous sulfate could occur during suicide attempts in adolescents or adults [7,8]. Recently, sodium ferrous citrate has also been widely used as an efficacious iron supplement for individuals with iron deficiency anemia or chronic kidney disease, with a slightly lower incidence of adverse effects than ferrous sulfate [9,10]. Here, we report autopsy findings in an adult case of acute iron poisoning

due to intentional overdose of sodium ferrous citrate.

The pathology of liver injury induced by ferrous sulfate has been documented as periportal or panlobular necrosis with hemorrhage or cholestasis [2,6,11]. Experimental studies of ferrous sulfate-induced liver damage in various animals confirmed that substantial necrosis of the liver parenchyma occurs similar to that in human cases and that extensive mitochondrial damage and changes in the activity of enzymes, such as glucose-6-phosphatase, are observed [2–4,12–14]. Although the basic mechanism of liver damage caused by either ferrous sulfate or ferrous citrate is most likely to be hydroxyl radical injury induced by the Fenton reaction or Haber-Weiss reaction [1,15], detailed pathological and molecular aspects of the injury, as well as stress responses of the liver cells and cell-type specificity of the liver injury, have yet to be

Abbreviations: ALT, alanine transaminase; AST, aspartate transaminase; CK19, cytokeratin 19; JNK, c-Jun N-terminal kinase; NTBI, nontransferrin-bound iron; RT-qPCR, quantitative reverse transcription-polymerase chain reaction; TNF- α , tumor necrosis factor- α ; UIBC, unbound iron binding capacity.

* Correspondence to: Division of Tumor Pathology, Department of Pathology, Asahikawa Medical University, Higashi 2-1-1-1, Midorigaoka, Asahikawa, Hokkaido 078-8510, Japan.

E-mail address: nishikwa@asahikawa-med.ac.jp (Y. Nishikawa).

<https://doi.org/10.1016/j.toxrep.2023.05.010>

Received 10 March 2023; Received in revised form 22 May 2023; Accepted 25 May 2023

Available online 30 May 2023

2214-7500/© 2023 The Authors. Published by Elsevier B.V. This is an open access article under the CC BY-NC-ND license (<http://creativecommons.org/licenses/by-nc-nd/4.0/>).

investigated.

Our human case demonstrated fulminant hepatic damage, pathologically characterized by an almost complete loss of hepatocytes, while bile duct cells were spared. Our experimentation indicated that acute overload of sodium ferrous citrate selectively injures hepatocytes without affecting the viability of bile duct cells and that hepatocyte injury is associated with DNA damage and a variety of stress responses.

2. Materials and methods

2.1. Analysis of a human case

An autopsy was performed two hours after the patient's death. No craniotomy was performed. Written informed consent was obtained from the patient's family before autopsy. The protocol for reporting this case was approved by the ethics committee of Asahikawa Medical University (approval number #17115, August 28, 2017). The systemic organs were removed, examined, and fixed in phosphate-buffered 10 % formalin. Tissues were processed to paraffin blocks and the Section (4 μ m) were subjected to hematoxylin and eosin staining, as well as Berlin blue staining. An autostainer (Leica Biosystems, Nußloch, Germany) was used to perform immunohistochemistry assessments of CD79a (antibody: M7050, DAKO, Carpinteria, CA), CD4 (antibody: NCL-L-CD4-1F6, Novocastra, Leica Microsystems, Wetzlar, Germany), CD8 (antibody: M7103, DAKO), HepPar1 (antibody: M7158, DAKO), cytokeratin 19 (CK19) (antibody: M0888, DAKO), and Ki-67 (MIB-1) (M7240, DAKO) expression.

2.2. Mouse model of acute iron poisoning

The protocols for animal experimentation were approved by the Animal Research Committee, Asahikawa Medical University (approval no. #16026, February 23, 2018), and all animal experiments adhered to the ARRIVE guidelines and the criteria outlined in the Guide for the Care and Use of Laboratory Animals prepared by the National Research Council. Male C57BL/6J mice (8–10 weeks old) were randomly divided into 6 groups (control [no treatment]; 3, 6, 12, 24, and 48 h following treatment) of 3 mice each. Immediately before administration, a powder formulation of sodium ferrous citrate (CID: 71587155; in Ferromia®, Eisai, Tokyo; containing 100 mg of iron in 1.2 g of powder) was dissolved in saline (180 mg/mL). The solution was administered orally to a dose of 250 mg of iron/kg. Mice were euthanized by overdoses of inhaled isoflurane.

2.3. Microscopic analyses and immunohistochemistry in the experimental studies

Livers were fixed with phosphate-buffered 4 % paraformaldehyde for 24 h, dehydrated, cleared, and embedded in paraffin. Immunohistochemical analyses were performed by the peroxidase method following an antigen retrieval procedure using Target Retrieval Solution, pH 6.0 (DAKO). The following antibodies were used: anti-cleaved caspase-3 (#9664, Cell Signaling Technology, Danvers, MA), anti-8-hydroxy-2'-deoxyguanosine (8-OHdG) (MOG-020 P, Japan Institute for the Control of Aging, NIKKEN SEIL), anti-SLC40A1 (ferroportin1) (BMP033, Medical and Biological Laboratories, Nagoya, Japan), anti-phosphorylated c-Jun (#9164, Cell Signaling Technology), anti-NF- κ B (p65) (sc109, Santa Cruz Biotechnology, Santa Cruz, CA), anti- γ H2AX (#2577, Cell Signaling Technology), anti-Myc (ab32072, Abcam, Cambridge, UK), anti-p53 (NCL-p53-CM5p), and anti-CK19 (gift of Dr. Atsushi Miyajima, The University of Tokyo).

2.4. Western blotting analysis

Protein samples (25 μ g of protein per lane) were subjected to SDS-PAGE and then transferred to polyvinylidene difluoride

membranes. The primary antibodies that were used included anti-phosphorylated c-Jun N-terminal kinase (JNK) (#9251, Cell Signaling Technology), anti-phosphorylated c-Jun (#9164, Cell Signaling Technology), and anti- β -actin (AC-15, Novus Biologicals, Littleton, CO). Detection was performed with ECL Prime Western Blotting Detection Reagent (GE Healthcare Bio-Sciences Corp., Piscataway, NJ).

2.5. Culture of hepatocytes and bile ducts

To compare the vulnerability of hepatocytes and bile duct cells to iron toxicity, we isolated and cultured these cells from intact mice or those treated with a lethal dose (600 mg/kg, p.o.) of sodium ferrous citrate 3 h prior to isolation. After the livers were enzymatically digested by the two-step collagenase perfusion technique, hepatocytes were collected and plated on collagen-coated dishes. The undigested fragments of Glisson's sheath containing bile duct cells were minced and embedded within a collagen gel matrix (Cellmatrix type I-A; Nitta Gelatin, Osaka, Japan). Cells were cultured in Williams' E medium supplemented with 10 mM nicotinamide, 10 % fetal bovine serum, 10 ng/mL epidermal growth factor, 10^{-7} M insulin, and 10^{-7} M dexamethasone. For bile duct cell cultures, 10 ng/mL tumor necrosis factor- α (TNF- α) (PeproTech Inc., Rocky Hill, NJ) was added to the medium.

2.6. Quantitative reverse transcription-polymerase chain reaction (RT-qPCR)

Total RNA was extracted from frozen mouse liver tissues and isolated cells and subjected to RT-qPCR analyses, which were performed using the $\Delta\Delta$ Ct method with FastStart Universal SYBR Green Master Mix (Roche Diagnostics, Mannheim, Germany). Each reaction was performed in duplicate, and the mRNA levels were normalized against the levels of glyceraldehyde-3-phosphate dehydrogenase (*Gapdh*). The specific primers used were as follows: hepcidin gene (*Hamp*) mRNA, forward 5'-AGGGCAAGACATTGCGATACC-3' and reverse 5'-TGCAACAGATACCACACTGGG-3'; ferroportin1 gene (*Slc40a1*), forward 5'-TGTGGAGGATGAAATGTGTAAC-3' and reverse 5'-TGAA-GAGCCACCATACACACA-3'; transferrin receptor type 2 gene (*Tfr2*) mRNA, forward 5'-AGCAATTCAGACCTCG-3' and reverse 5'-TTGAGGTGTAGCAGCTGAG-3'; divalent metal transporter 1 gene (*Dmt1*) mRNA, forward 5'-TGCTGAGCGAAGATACCAGC-3' and reverse 5'-CTCTGATGGCTCCCTGCAAA-3'; a metal cation symporter gene (*Zip14*) mRNA, forward 5'-GGCTGGAGGACTTCAGTGTG-3' and reverse 5'-GGTGGAGCCAAGGCTAATGT-3'; *Gapdh* mRNA, forward 5'-ACCA-CAGTCCATGCCATCAC-3' and reverse 5'-TCCACCACCCTGTGCTGA-3'.

3. Results

3.1. Clinical summary of the human case

A 39-year-old woman with a history of iron-deficiency anemia was transported to the Emergency Department of our hospital by ambulance because of the development of severe disturbance of consciousness (Glasgow Coma Scale: 8; Japan Coma Scale: 100) after she intentionally consumed a large amount of sodium ferrous citrate tablets (equivalent to 7.5 g of iron), which had been prescribed for oral iron preparation. On physical examination, substantial gastrointestinal hemorrhage was noted. Her blood pressure was 143/66 mmHg, her body temperature was 35.7 °C, and her heart rate was 32/min. Repeated gastric and intestinal lavages were performed. A chelating agent deferoxamine mesylate was administered, and plasma exchange was performed for the initial 3 days without any meaningful improvements in her clinical status.

The plasma levels of alanine transaminase (ALT) and aspartate transaminase (AST) abruptly increased on Day 2 (> 15,000 IU/L), followed by a rapid decline to the basal level (Fig. 1a). The levels of total

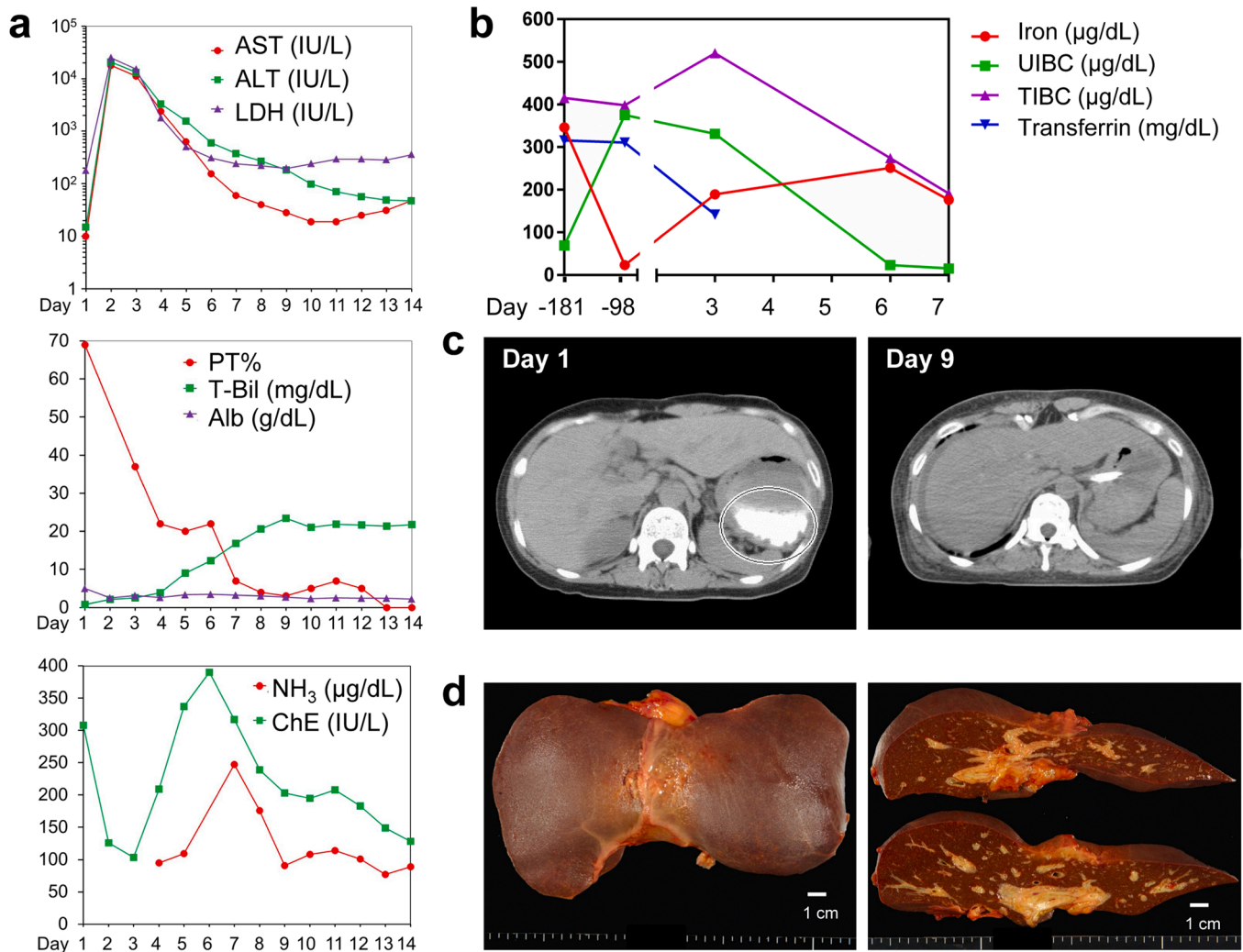


Fig. 1. Fulminant liver failure induced by an overdose of ferrous citrate in a 39-year-old woman. **a** Time course of laboratory values indicating liver functions following the incident; **b** Plasma iron, total iron binding capacity (TIBC), unbound iron binding capacity (UIBC), and transferrin before and after the incident; **c** Abdominal CT images at Day 1 and Day 9; **d** Gross photographs of the liver at autopsy.

bilirubin gradually increased and reached more than 20 mg/dL on Day 9, whereas prothrombin time decreased rapidly, and the plasma albumin levels were constantly low (Fig. 1a). The plasma iron levels were high on Day 3 (189 mg/dL on day; reference range: 50–155) and further increased on Day 6 with a concomitant decrease in unbound iron binding capacity (UIBC) (Fig. 1b). The plasma level of ferritin was 506.1 ng/mL (reference range: 6.4–144.4) on Day 3. There was a rapid increase in the levels of pancreatic enzymes on Day 4, suggesting acute pancreatitis. No abnormal findings were noted in abdominal computed tomography images obtained on Day 1, except for a radiodense content in the stomach (Fig. 1c). However, severe atrophy of the liver parenchyma became evident on Day 9 (Fig. 1c). The patient died of fulminant hepatic failure associated with acute pancreatitis and intestinal hemorrhage on Day 13. Two hours later, an autopsy was performed.

3.2. Autopsy findings of the case

Severe jaundice of the skin and sclerae was noted. There was mild edema in the extremities, and the body weight was 50.5 kg. The liver was small (389 g) without distinct regenerative nodules (Fig. 1d). The cut surfaces demonstrated dark-brown discoloration with condensation of the porto-venous radicals (Fig. 1d). Microscopically, the hepatic capsule was wrinkled due to severe atrophy of the liver parenchyma (Fig. 2a) with a virtually complete disappearance of hepatocytes

(Fig. 2b, c). A small number of minute clusters of hepatocytes were found in a limited area of the right lobe (Fig. 2d). Berlin blue staining did not demonstrate any stored iron throughout the liver parenchyma (Fig. 2e), possibly due to the use of deferoxamine mesylate. There were many macrophages containing brown pigments that were negative for Berlin blue staining (Fig. 2c, e). The bile ducts and ductules in the portal area appeared to be viable with slightly large and hyperchromatic nuclei, suggesting a reactive change (Fig. 2f). There was marked periportal infiltration of inflammatory cells, mainly comprising plasma cells and lymphocytes (Fig. 2b). The phenotypes of lymphocytes were mixed, including scattered CD-79a-positive B cells and densely infiltrated T cells, positive for either CD4 or CD8 (Fig. 2g-i). Clusters of the surviving hepatocytes were highlighted by HepPar1 staining (Fig. 2j, k). These hepatocytes were MIB-1-negative, indicating that they lacked regenerative activity (Fig. 2l). In contrast, bile duct structures remained intact and appeared to be rather condensed (Fig. 2m, n). Some of the ductal cells were MIB-1-positive (Fig. 2o).

Significant autopsy findings of the other organs were as follows. Mucosa of the gastrointestinal tract was edematous, and the small intestine showed mild mucosal hemorrhage. The lungs (left, 303 g; right, 400 g) showed diffuse alveolar hemorrhage (Fig. 3a, b), which was associated with neutrophilic infiltration (Fig. 3c). There was necrosis of the parenchyma and surrounding fat in the head of the pancreas (Fig. 3d). Acinar atrophy and stromal fibrosis were found in the

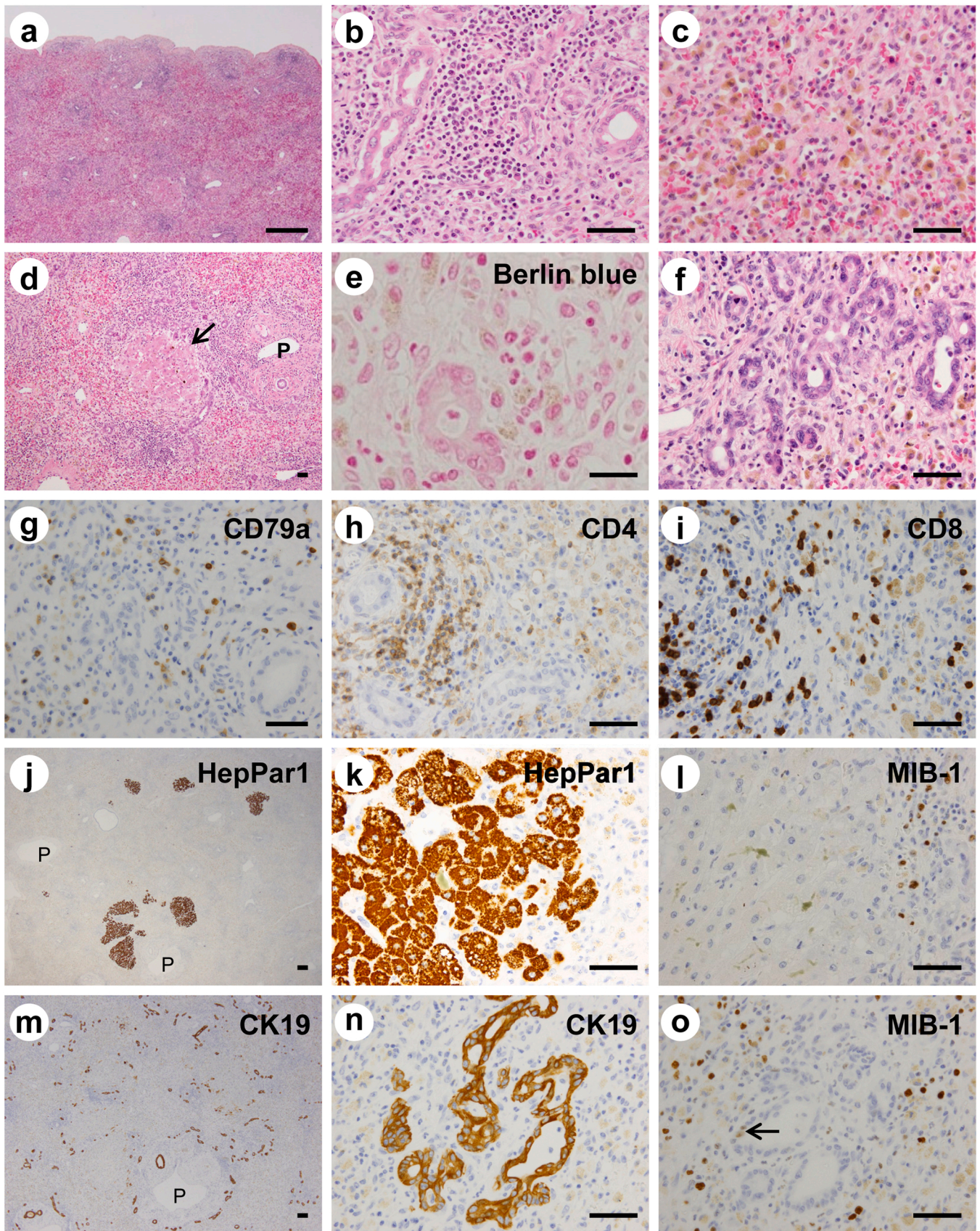


Fig. 2. Histological and immunohistochemical findings of the liver obtained at autopsy. **a–d, f** Hematoxylin and eosin staining; **e** Berlin blue staining; **g–o** Immunohistochemistry for markers for lymphocytes (CD79a, CD4, and CD8), hepatocytes (HepPar1), bile ducts (CK19), and cellular proliferation (MIB-1). The arrow in **d** indicates a cluster of remaining hepatocytes. The arrows in **o** indicate MIB-1-positive nuclei in bile duct cells. P: portal vein. Scale bars = 500 μm (a), 50 μm (b–o).

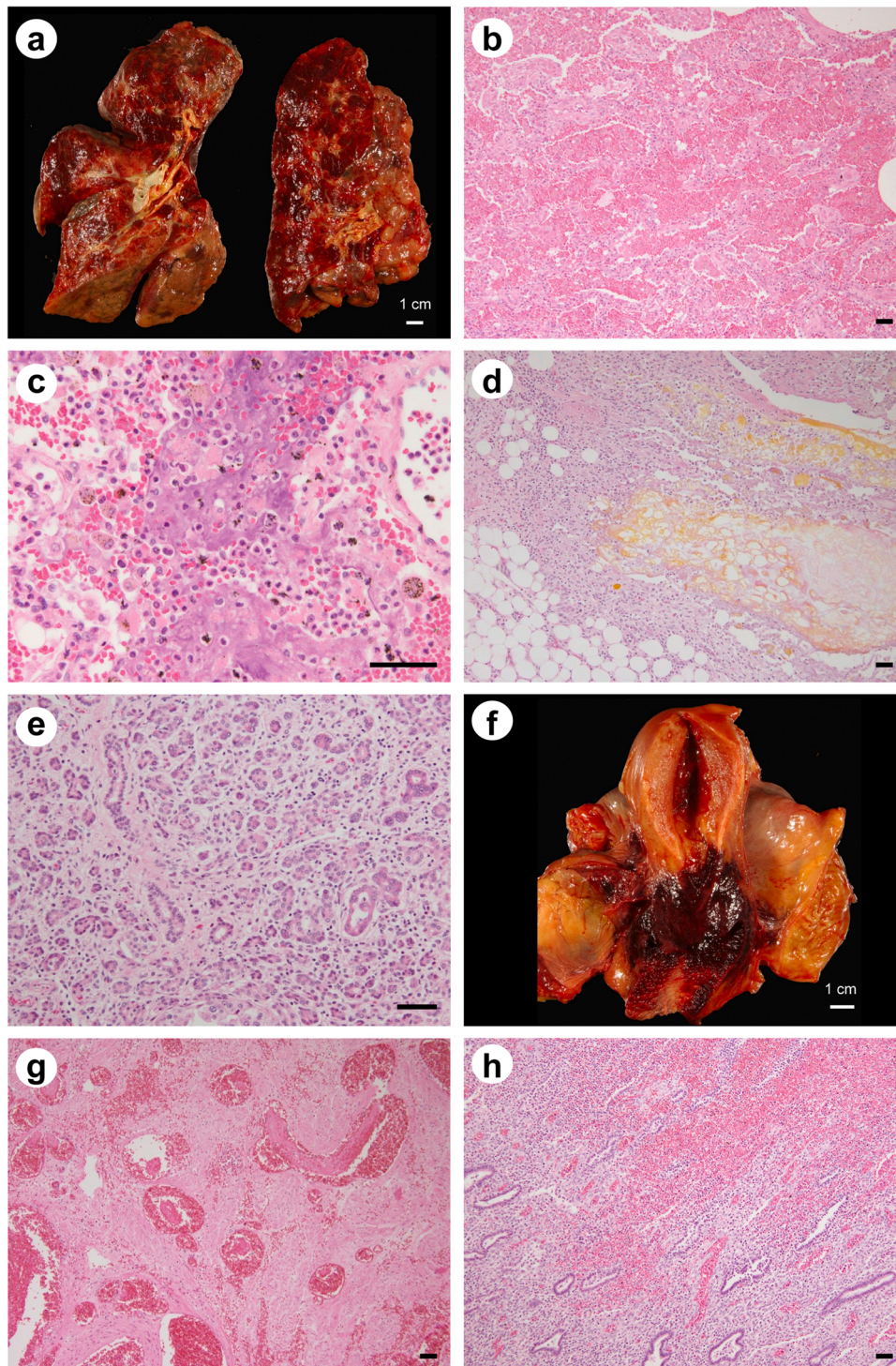


Fig. 3. Gross and histological findings of the other systemic organs. **a, f** Gross photographs of the lungs (**a**) and uterus (**f**) at autopsy; **b–e, g, h** Hematoxylin and eosin staining of the lung (**b, c**), pancreas (**d, e**), uterine cervix (**g**), and endometrium (**h**). Scale bars = 50 μ m (**b–e, g, h**).

remaining parenchyma (Fig. 3e). The uterine cervix and vagina were massively hemorrhagic (Fig. 3f, g) and the endometrium was in the menstrual phase (Fig. 3h).

3.3. Liver injury induced by acute sodium ferrous citrate overload in mice

To assess the detailed pathobiological features of acute liver injury induced by iron overload, a sodium ferrous citrate (Ferromia®) suspension was administered by gavage to mice at a dose of 250 mg of iron

per kg of body weight. The plasma concentration of iron reached the maximum level (1500 μ g/dL) at 3 h after administration, followed by a gradual decline (Fig. 4a). The plasma levels of AST and ALT markedly increased at 6 h (3000 IU/L) after administration and then rapidly declined to basal levels (Fig. 4a).

Histologically, the nuclei of hepatocytes became pyknotic and began to disintegrate specifically in the periportal region after 6 h, and these changes were more evident thereafter (Fig. 4b). The accumulation of ferric iron in the periportal hepatocytes, which were positively stained

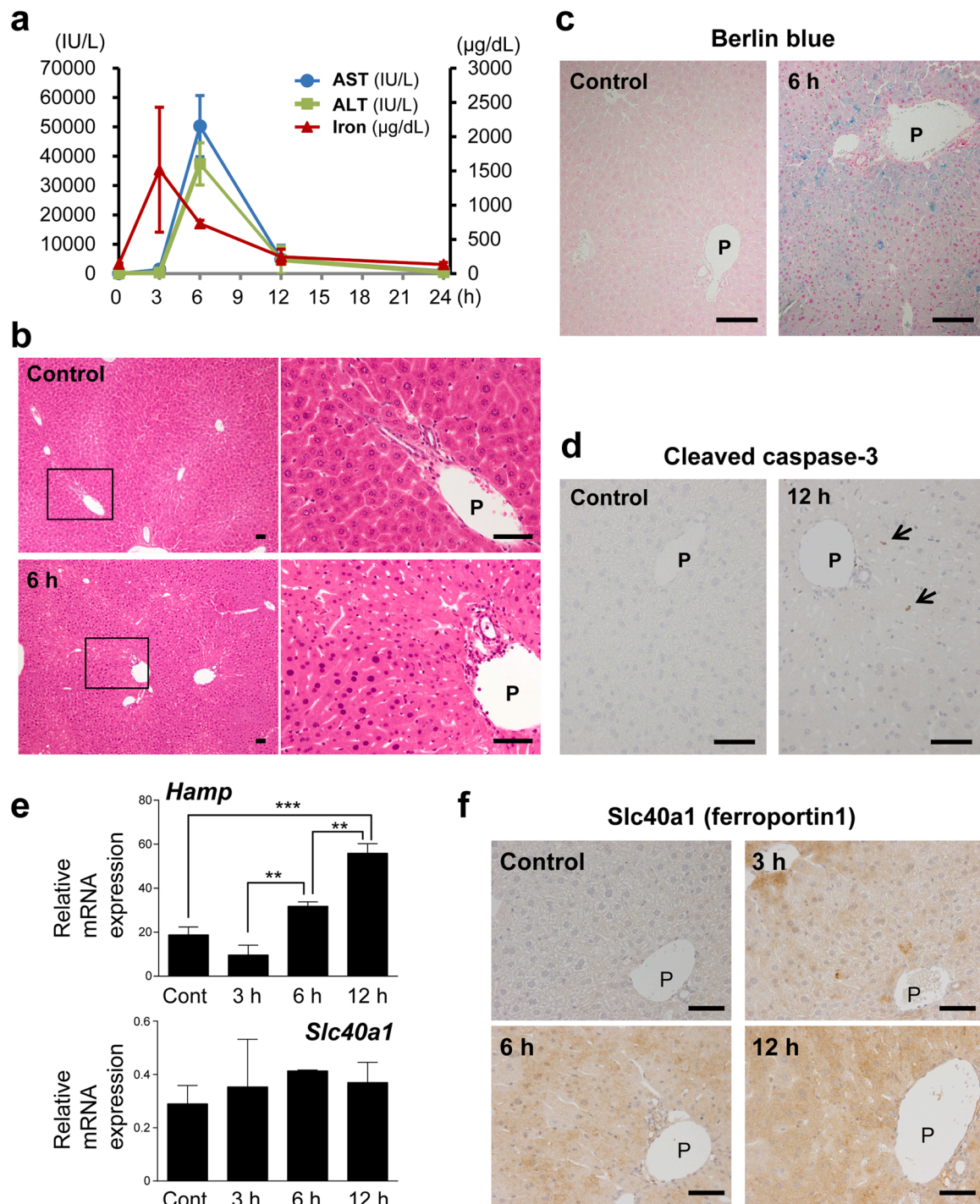


Fig. 4. Severe liver damage induced by ferrous citrate in mice. Mice were treated with 250 mg of iron per kg of body weight (p.o.). **a** Time course of plasma AST, ALT, and iron levels; **b** Hematoxylin and eosin staining; **c** Berlin blue staining; **d** Immunohistochemistry for cleaved caspase-3 expression; **e** RT-qPCR for estimation of the levels of *Hamp* and *Slc40a2* mRNA; **f** Immunohistochemistry for *Slc40a1* (ferroportin1) expression. The arrows in **d** indicate cleaved caspase-3-positive hepatocytes. The error bars indicate the means \pm SEMs; $n = 3$ replicates (**a**, **e**); analyzed by one-way analysis of variance (ANOVA). (**e**), $**P < 0.01$, $***P < 0.005$. P: portal vein. Scale bars = 50 μm (**b–d**, **f**).

with Berlin blue, was evident as early as 3 h and became most prominent at 6 h following administration (Fig. 4c). Only a few cleaved caspase-3-positive apoptotic cells were found in the injured area throughout the observation period (Fig. 4d).

In response to acute intracellular iron accumulation, the mRNA expression of the hepcidin gene (*Hamp*) was significantly increased after 6 h (Fig. 4e). Although the levels of ferroportin1 gene (*Slc40a1*) mRNA were unchanged (Fig. 4e), immunohistochemical analysis revealed

increased expression of ferroportin1 protein in hepatocytes as early as 3 h after treatment (Fig. 4f).

3.4. Responses to cellular stress and DNA injury following acute sodium ferrous citrate overload

Ferrous iron accumulated in hepatocytes is expected to generate extremely reactive hydroxyl radicals, which oxidatively damage various

macromolecules including nucleic acids. Immunohistochemistry for 8-OHdG demonstrated that iron overload induced nuclear accumulation of this oxidized nucleoside in hepatocytes, as well as in bile duct cells (Fig. 5a). We then examined responses to oxidative stress in the liver. The levels of phosphorylated JNK, a stress kinase, started to increase at 3 h following iron overload, peaked at 6 h, and then returned to basal levels (Fig. 5b). Its downstream effector, c-Jun, was strongly phosphorylated from 3 to 12 h following iron overload (Fig. 5b). Immunohistochemically, hepatocytes in the intact liver were negative for phosphorylated c-Jun, although the nuclei of some bile ducts were weakly positive (Fig. 5c). However, phosphorylated c-Jun became detectable in hepatocytic nuclei at 3 h following iron overload, with a further increase in immunoreactivity in bile ducts (Fig. 5c). We also examined the expression of NF- κ B, which is known to be activated by cellular stress, especially that incurred by hydroxyl radicals [16]. NF- κ B staining was negative in hepatocytes in the intact liver, but the immunoreactivity was not affected by iron overload (Fig. 5c). In contrast, clusters of NF- κ B-positive Kupffer cells appeared at 3 h following iron overload; the clusters were distributed throughout the hepatic lobule thereafter (Fig. 5c). We also examined the expression of γ -H2AX, which is recruited to double-strand breaks of DNA. γ -H2AX expression was first detected in the nuclei of periportal hepatocytes after 6 h but not in other types of cells (Fig. 5c).

We then examined the expression of Myc and p53, which are known to be involved in the tissue response to cellular injury. At 6 h following iron overload, nuclear Myc expression was detected in bile duct cells and some sinusoidal cells, as well as in some periportal hepatocytes (Fig. 5d). After 12 h, most of the damaged periportal hepatocytes demonstrated strong immunoreactivity for Myc (Fig. 5d). Although p53 expression was barely detected in either hepatocytes or nonparenchymal cells until 12 h following iron overload, it was expressed in the nuclei of damaged periportal hepatocytes after 24 h (Fig. 5d).

3.5. Sparing of bile ducts in iron-induced acute liver injury

After 24 h, patchy areas of necrosis were grossly apparent as discolored zones. Microscopically, the necrotic areas contained the portal tract associated with mild inflammatory cell infiltration (Fig. 6a), where bile ducts, which were highlighted by CK19 immunohistochemistry, appeared to be intact (Fig. 6b).

To confirm that the iron-induced injury is hepatocyte-specific, we isolated hepatocytes and portal tract containing bile ducts from the liver 3 h after treatment with a lethal dose of sodium ferrous citrate. Hepatocytes from the intact mice formed monolayers soon after plating, and those from the iron-treated livers did not attach to collagen-coated plastic surfaces and instead freely floated in the medium (Fig. 6c). This finding indicated that the death process that occurred in hepatocytes might have been completed soon after exposure to the lethal dose of iron. In contrast, the portal tract tissues containing bile ducts, either from control livers or iron-treated livers, showed extensive branching morphogenesis, which was augmented by TNF- α (Fig. 6c).

To examine whether the cell type-specificity of iron-induced injury might be related to the differences in the expression levels of receptors or transporter proteins involved in iron uptake or excretion, the mRNA expression levels of the genes for transferrin receptor 2 (*Tfr2*), divalent metal transporters (*Dmt1* and *Zip14*), ferroportin1 (*Slc40a1*), and hepcidin (*Hamp*) were compared between isolated hepatocytes and portal tract containing bile ducts. Although *Tfr2* and *Hamp* mRNA expression was significantly higher in hepatocytes, as expected, there were no significant differences in the expression levels of the divalent metal transporters and *Slc40a1* between hepatocytes and the portal tract (Fig. 6d).

4. Discussion

Whereas all previously published reports, either human or

experimental, described liver injury due to overdoses of ferrous sulfate, our study also demonstrates that similarly substantial levels of liver necrosis could be induced by sodium ferrous citrate. Although the plasma iron concentration immediately after intentional ingestion of sodium ferrous citrate was not available in our case, the equivalent dose of sodium ferrous citrate in mice elevated their plasma iron concentrations to 1500 μ g/dL after 3 h, which surpasses the reported level (1000 μ g/dL) that could induce severe liver injury [1].

In our human case, almost all the hepatocytes disappeared and regenerative changes in the residual hepatocytes were minimal. In mice, the hepatocyte viability was completely lost at 3 h following a lethal dose (600 mg/kg, p.o.) of sodium ferrous citrate. Although we could not demonstrate actually occurred iron accumulation in hepatocytes, which is a limitation of our analyzes, this case and our experimental results highlight how deleterious is the overdosed iron. Sodium ferrous citrate has been shown to be more readily absorbed by the intestines as compared with ferrous sulfate, since the former is present in the intestines as a low-molecular weight chelated iron complex, while the latter forms insoluble high-molecular weight polymers [17,18]. Mouse experiments demonstrated that sodium ferrous citrate induces liver damage with a periportal prevalence of parenchymal injury. The zonal distribution of the injury could be explained by the proximity of the periportal hepatocytes to the branches of portal veins [2]. Damaged hepatocytes did not show typical characteristics of apoptotic cell death, suggesting that they underwent necrosis. Although the possibility of ferroptosis [19], an iron-dependent nonapoptotic cell death, should also be considered, the marked accumulation of 8-OHdG in the nuclei of the dying hepatocytes highly suggests oxidative stress, therefore the cell death is most likely induced by an increase in H₂O₂ dependent, iron-catalyzed hydroxyl radical production [20].

Interestingly, ferroportin1 protein expression, but not its mRNA expression, was significantly augmented in response to iron accumulation. Ferroportin1 is known to be the transporter of iron released by enterocytes, macrophages, and hepatocytes [21]. Although it has been shown to be endocytosed and degraded with the interaction of hepcidin produced by hepatocytes [22,23], the increased expression preceded the increase in *Hamp* mRNA levels. The 5'-untranslated region of the ferroportin1 gene (*Slc40a1*) contains iron-response elements, and its translation has been demonstrated to be augmented when iron is abundant [24–26]. Our findings suggest that hepatocytes might have a self-protecting mechanism to immediately commence iron exportation in response to intracellular iron accumulation.

When transferrin is saturated during iron overload, nontransferrin-bound iron (NTBI) appears in the plasma and exerts various toxic effects due to the generation of reactive oxygen species that cause injury of plasma membranes and intracellular organelles [27]. Intracellular NTBI is loosely bound to small molecular compounds, such as citrate [27]. Experimentally, injection of sodium ferrous citrate into the rat substantia nigra has been applied to induce nigral degeneration [28]. The toxicity of NTBI is considered to be mediated by hydroxyl radicals [1], which cause single- and double-strand breaks in DNA [29,30], as evidenced by γ -H2AX immunohistochemistry.

We demonstrated that the JNK-c-Jun pathway, which is rapidly activated by oxidative stress [31,32], is also activated by acute iron overload. This pathway has been shown to facilitate hepatocyte death induced by oxidative stress [33]. Another stress-associated protein, NF- κ B, was activated in Kupffer cells but not in hepatocytes, which is compatible with a previous in vitro study showing that ferrous iron activates NF- κ B and releases tumor necrosis factor- α , thereby further exacerbating liver injury [34]. Our study also demonstrated that iron overload induces increased expression of Myc and p53, which are known to be involved in the cellular response to oxidative stress [35]. The early transient Myc expression in bile duct cells might represent a reactive response, since Myc has been shown to be activated in bile duct cells during cholestasis [36]. Myc has been shown to be phosphorylated at serine 62 and stabilized when cells are subjected to oxidative stress [37,

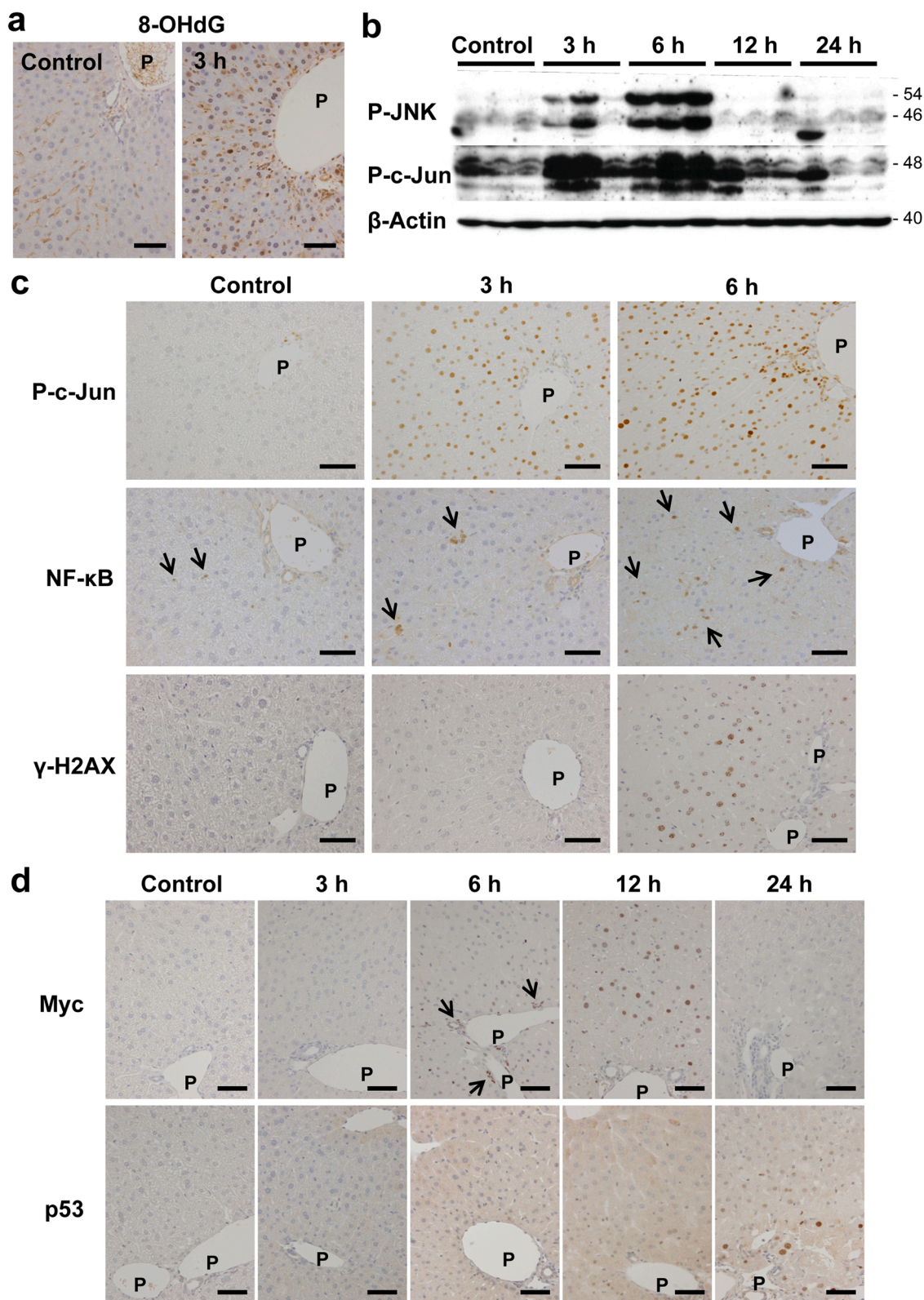


Fig. 5. Tissue response of the liver following administration of ferrous citrate. Mice were treated with 250 mg of iron per kg of body weight (p.o.). **a** Immunohistochemistry for 8-OHdG; **b** Western blot analyses for the expression of phosphorylated JNK and phosphorylated c-Jun; **c** Immunohistochemistry for the expression of phosphorylated c-Jun, NF-κB, and γ-H2AX in the liver; **d** Immunohistochemistry for the expression of Myc and p53 in the liver. The arrows in **c** indicate NF-κB-positive Kupffer cells. The arrows in **d** indicate Myc-positive bile duct cells. P: portal vein. Scale bars = 50 μm (a, c, d).

ferrous citrate in a human autopsy case and studied its hepatocyte-specific deleterious effects, as well as tissue responses, in mouse experiments. Our work highlights the danger of acute sodium ferrous citrate toxicity and calls attention to a lethal outcome of this commonly prescribed iron supplement when overdosed.

CRedit authorship contribution statement

YNi performed the autopsy, performed the experimental studies, interpreted the data, and was a major contributor to writing the manuscript. YM, RW, MMi, MMa, YNa, HT, MG, and YO performed the experimental studies and interpreted the data. SF managed the patient and provided clinical information. All authors were involved in the critical review of the manuscript and approved the final version.

Funding

This study was supported by grants from the Japan Society for the Promotion of Science (#25670186).

Declaration of Competing Interest

The authors declare that they have no known competing financial interests or personal relationships that could have appeared to influence the work reported in this paper.

Data Availability

Data will be made available on request.

Acknowledgments

We thank Dr. Tetsushi Yamamoto for providing clinical information and Mr. Yoshiyasu Satake for technical assistance.

Appendix A. Supporting information

Supplementary data associated with this article can be found in the online version at [doi:10.1016/j.toxrep.2023.05.010](https://doi.org/10.1016/j.toxrep.2023.05.010).

References

- [1] A. Robertson, M. Tenenbein, Hepatotoxicity in acute iron poisoning, *Hum. Exp. Toxicol.* 24 (2005) 559–562, <https://doi.org/10.1191/0960327105ht5640a>.
- [2] M.A. Luongo, S.S. Bjornson, The liver in ferrous sulfate poisoning: a report of three fatal cases in children and an experimental study, *N. Engl. J. Med.* 251 (1954) 995–999, <https://doi.org/10.1056/NEJM195412162512501>.
- [3] R.J. Brown, J.D. Gray, The mechanism of acute ferrous sulphate poisoning, *Can. Med. Assoc. J.* 73 (1955) 192–197.
- [4] C.F. Whitten, G.W. Gibson, M.H. Good, J.F. Goodwin, A.J. Brough, Studies in acute iron poisoning. I. Desferrioxamine in the treatment of acute iron poisoning: clinical observations, experimental studies, and theoretical considerations, *Pediatrics* 36 (1965) 322–335.
- [5] F.J. deCastro, R. Jaeger, W.A. Gleason Jr., Liver damage and hypoglycemia in acute iron poisoning, *Clin. Toxicol.* 10 (1977) 287–289, <https://doi.org/10.3109/15563657708992425>.
- [6] W.A. Gleason Jr., D.E. deMello, F.J. deCastro, J.J. Connors, Acute hepatic failure in severe iron poisoning, *J. Pediatr.* 95 (1979) 138–140, [https://doi.org/10.1016/s0022-3476\(79\)80108-0](https://doi.org/10.1016/s0022-3476(79)80108-0).
- [7] S.R. Daram, P.H. Hayashi, Acute liver failure due to iron overdose in an adult, *South Med. J.* 98 (2005) 241–244, <https://doi.org/10.1097/01.SMJ.0000152546.05519.FE>.
- [8] J. Lai, J. Chu, R. Amon, Pediatric liver transplantation for fulminant hepatic failure secondary to intentional iron overdose, *Pediatr. Transpl.* 21 (2017), <https://doi.org/10.1111/ptr.12994>.
- [9] R. Womack, F. Berru, B. Panwar, O.M. Gutierrez, Effect of ferric citrate versus ferrous sulfate on iron and phosphate parameters in patients with iron deficiency and CKD: a randomized trial, *Clin. J. Am. Soc. Nephrol.* 15 (2020) 1251–1258, <https://doi.org/10.2215/CJN.15291219>.
- [10] G.A. Block, S. Fishbane, M. Rodriguez, G. Smits, S. Shemesh, P.E. Pergola, M. Wolf, G.M. Chertow, A 12-week, double-blind, placebo-controlled trial of ferric citrate for the treatment of iron deficiency anemia and reduction of serum phosphate in patients with CKD Stages 3–5, *Am. J. Kidney Dis.* 65 (2015) 728–736, <https://doi.org/10.1053/j.ajkd.2014.10.014>.
- [11] J.P. Pestaner, K.G. Ishak, F.G. Mullick, J.A. Centeno, Ferrous sulfate toxicity: a review of autopsy findings, *Biol. Trace Elem. Res.* 69 (1999) 191–198, <https://doi.org/10.1007/BF02783871>.
- [12] C.L. Witzleben, N.J. Chaffey, Acute ferrous sulfate poisoning. A histochemical study of its effect on the liver, *Arch. Pathol.* 82 (1966) 454–461.
- [13] C.L. Witzleben, An electron microscopic study of ferrous sulfate induced liver damage, *Am. J. Pathol.* 49 (1966) 1053–1067.
- [14] C.E. Ganote, G. Nahara, Acute ferrous sulfate hepatotoxicity in rats. An electron microscopic and biochemical study, *Lab. Invest.* 28 (1973) 426–436.
- [15] G. Papanikolaou, K. Pantopoulos, Iron metabolism and toxicity, *Toxicol. Appl. Pharm.* 202 (2005) 199–211, <https://doi.org/10.1016/j.taap.2004.06.021>.
- [16] X. Shi, Z. Dong, C. Huang, W. Ma, K. Liu, J. Ye, F. Chen, S.S. Leonard, M. Ding, V. Castranova, V. Vallyathan, The role of hydroxyl radical as a messenger in the activation of nuclear transcription factor NF-kappaB, *Mol. Cell. Biochem.* 194 (1999) 63–70.
- [17] K. Terato, T. Fujita, Y. Yoshino, Studies on iron absorption. I. The role of low molecular polymer in iron absorption, *Am. J. Dig. Dis.* 18 (1973) 121–128, <https://doi.org/10.1007/BF01073155>.
- [18] K. Terato, Y. Hiramoto, Y. Yoshino, Studies on iron absorption. II. Transport mechanism of low molecular iron chelate in rat intestine, *Am. J. Dig. Dis.* 18 (1973) 129–134, <https://doi.org/10.1007/BF01073156>.
- [19] S. Toyokuni, I. Yanatori, Y. Kong, H. Zheng, Y. Motooka, L. Jiang, Ferroptosis at the crossroads of infection, aging and cancer, *Cancer Sci.* 111 (2020) 2665–2671, <https://doi.org/10.1111/cas.14496>.
- [20] S.J. Dixon, K.M. Lemberg, M.R. Lamprecht, R. Skouta, E.M. Zaitsev, C.E. Gleason, D.N. Patel, A.J. Bauer, A.M. Cantley, W.S. Yang, B. Morrison 3rd, B.R. Stockwell, Ferroptosis: an iron-dependent form of nonapoptotic cell death, *Cell* 149 (2012) 1060–1072, <https://doi.org/10.1016/j.cell.2012.03.042>.
- [21] A. Donovan, C.A. Lima, J.L. Pinkus, G.S. Pinkus, L.I. Zon, S. Robine, N.C. Andrews, The iron exporter ferroportin/Slc40a1 is essential for iron homeostasis, *Cell Metab.* 1 (2005) 191–200, <https://doi.org/10.1016/j.cmet.2005.01.003>.
- [22] E. Nemeth, M.S. Tuttle, J. Powelson, M.B. Vaughn, A. Donovan, D.M. Ward, T. Ganz, J. Kaplan, Hepcidin regulates cellular iron efflux by binding to ferroportin and inducing its internalization, *Science* 306 (2004) 2090–2093, <https://doi.org/10.1126/science.1104742>.
- [23] B. Qiao, P. Sugianto, E. Fung, A. Del-Castillo-Rueda, M.J. Moran-Jimenez, T. Ganz, E. Nemeth, Hepcidin-induced endocytosis of ferroportin is dependent on ferroportin ubiquitination, *Cell Metab.* 15 (2012) 918–924, <https://doi.org/10.1016/j.cmet.2012.03.018>.
- [24] S. Abboud, D.J. Haile, A novel mammalian iron-regulated protein involved in intracellular iron metabolism, *J. Biol. Chem.* 275 (2000) 19906–19912, <https://doi.org/10.1074/jbc.M000713200>.
- [25] A. Lymboussaki, E. Pignatti, G. Montosi, C. Garuti, D.J. Haile, A. Pietrangelo, The role of the iron responsive element in the control of ferroportin1/IREG1/MTP1 gene expression, *J. Hepatol.* 39 (2003) 710–715, [https://doi.org/10.1016/s0168-8278\(03\)00408-2](https://doi.org/10.1016/s0168-8278(03)00408-2).
- [26] A.T. McKie, P. Marciani, A. Rolfs, K. Brennan, K. Wehr, D. Barrow, S. Miret, A. Bomford, T.J. Peters, F. Farzaneh, M.A. Hediger, M.W. Hentze, R.J. Simpson, A novel duodenal iron-regulated transporter, IREG1, implicated in the basolateral transfer of iron to the circulation, *Mol. Cell* 5 (2000) 299–309, [https://doi.org/10.1016/s1097-2765\(00\)80425-6](https://doi.org/10.1016/s1097-2765(00)80425-6).
- [27] P. Brissot, M. Ropert, C. Le Lan, O. Loreal, Non-transferrin bound iron: a key role in iron overload and iron toxicity, *Biochim. Biophys. Acta* 1820 (2012) 403–404.
- [28] K.P. Mohanakumar, A. de Bartolomeis, R.M. Wu, K.J. Yeh, L.M. Sternberger, S. Y. Peng, D.L. Murphy, C.C. Chiueh, Ferrous-citrate complex and nigral degeneration: evidence for free-radical formation and lipid peroxidation, *Ann. N. Y. Acad. Sci.* 738 (1994) 392–399, <https://doi.org/10.1111/j.1749-6632.1994.tb21828.x>.
- [29] D.R. Lloyd, P.L. Carmichael, D.H. Phillips, Comparison of the formation of 8-hydroxy-2'-deoxyguanosine and single- and double-strand breaks in DNA mediated by fenton reactions, *Chem. Res. Toxicol.* 11 (1998) 420–427, <https://doi.org/10.1021/tx970156l>.
- [30] D. Pra, S.I. Franke, J.A. Henriques, M. Fenech, Iron and genome stability: an update, *Mutat. Res.* 733 (2012) 92–99, <https://doi.org/10.1016/j.mrfmmm.2012.02.001>.
- [31] V. Adler, A. Schaffer, J. Kim, L. Dolan, Z. Ronai, UV irradiation and heat shock mediate JNK activation via alternate pathways, *J. Biol. Chem.* 270 (1995) 26071–26077, <https://doi.org/10.1074/jbc.270.44.26071>.
- [32] K.G. Mendelson, L.R. Contois, S.G. Tevosian, R.J. Davis, K.E. Paulson, Independent regulation of JNK/p38 mitogen-activated protein kinases by metabolic oxidative stress in the liver, *Proc. Natl. Acad. Sci. USA* 93 (1996) 12908–12913, <https://doi.org/10.1073/pnas.93.23.12908>.
- [33] M.J. Czaja, Cell signaling in oxidative stress-induced liver injury, *Semin. Liver Dis.* 27 (2007) 378–389, <https://doi.org/10.1055/s-2007-991514>.
- [34] H. She, S. Xiong, M. Lin, E. Zandi, C. Giulivi, H. Tsukamoto, Iron activates NF-kappaB in Kupffer cells, *Am. J. Physiol. Gastrointest. Liver Physiol.* 283 (2002) G719–G726, <https://doi.org/10.1152/ajpgi.00108.2002>.
- [35] J.M. Mates, J.A. Campos-Sandoval, J. de Los Santos-Jimenez, J. Marquez, Glutaminases regulate glutathione and oxidative stress in cancer, *Arch. Toxicol.* 94 (2020) 2603–2623, <https://doi.org/10.1007/s00204-020-02838-8>.
- [36] T.F. Tracy Jr., M.E. Goerke, P.V. Bailey, C. Sotelo-Avila, T.R. Weber, Growth-related gene expression in early cholestatic liver injury, *Surgery* 114 (1993) 532–537, [https://doi.org/10.1007/s0039-6060\(93\)90289-P](https://doi.org/10.1007/s0039-6060(93)90289-P).

- [37] B. Benassi, M. Fanciulli, F. Fiorentino, A. Porrello, G. Chiorino, M. Loda, G. Zupi, A. Biroccio, c-Myc phosphorylation is required for cellular response to oxidative stress, *Mol. Cell* 21 (2006) 509–519, <https://doi.org/10.1016/j.molcel.2006.01.009>.
- [38] X. Wang, M. Cunningham, X. Zhang, S. Tokarz, B. Laraway, M. Troxell, R.C. Sears, Phosphorylation regulates c-Myc's oncogenic activity in the mammary gland, *Cancer Res.* 71 (2011) 925–936, <https://doi.org/10.1158/0008-5472.CAN-10-1032>.
- [39] D.P. Waterman, J.E. Haber, M.B. Smolka, Checkpoint responses to DNA double-strand breaks, *Annu. Rev. Biochem.* 89 (2020) 103–133, <https://doi.org/10.1146/annurev-biochem-011520-104722>.
- [40] G.S. Wu, The functional interactions between the p53 and MAPK signaling pathways, *Cancer Biol. Ther.* 3 (2004) 156–161, <https://doi.org/10.4161/cbt.3.2.614>.
- [41] M.J. Wood, V.L. Gadd, L.W. Powell, G.A. Ramm, A.D. Clouston, Ductular reaction in hereditary hemochromatosis: the link between hepatocyte senescence and fibrosis progression, *Hepatology* 59 (2014) 848–857, <https://doi.org/10.1002/hep.26706>.